Journal of Superconductivity and Novel Magnetism
https://doi.org/10.1007/s10948-023-06567-8

ORIGINAL PAPER

Phases, Microstructure and Magnetic Properties in a Severely Deformed Cr-Ni–Al Alloy

Ludmila I. Kveglis[1] · Dosym E. Yerbolatuly[2] · Fedor M. Noskov[1] · Sergey V. Komogortsev[3] · Mikhail N. Volochaev[3]

Received: 24 February 2023 / Accepted: 14 April 2023

Abstract
The phases, microstructure, and magnetic properties in a severely deformed Cr-Ni–Al alloy have been studied. The eutectic microstructure observed in localized regions of the alloy can be interpreted as a result from the super-Arrhenius relaxation of the alloy. According to X-ray diffraction and magnetometry, the nanosized nickel inclusions in the matrix of the chromium-nickel γ-solid solution are formed. It is shown that, after severe (superplastic) deformation, a unidirectional magnetic anisotropy is induced, which may be associated with the antiferromagnetic coupling between the $CrNi_2$ matrix and the nickel inclusions.

Keywords Nickel–chromium alloy · Coercive force · Magnetic anisotropy · Super-plasticity · Intermetallic phases

1 Introduction

At the moment, the development of metal-intermetallic alloys is of particular relevance in the areas of aircraft and shipbuilding, the chemical industry, instrument making, space technology, etc. In addition to high mechanical properties, parts of these industries are often subject to special requirements. In some cases, the non-magnetic behavior high corrosion resistance and fatigue strength under contact loading are desired simultaneously. These requirements are met by the high-chromium precipitation-hardening Cr-Ni–Al alloy 40HNU [1, 2]. This heat-resistant nickel–chromium-based alloy (Cr—39.5%; Al—3.75%; C—0.015%; the rest is Ni) is a promising material, because of its high hardness, not inferior to hardened steels (up to 60 Rockwell units) and, at the same time, low magnetic susceptibility (no more than 3.5×10^{-6} cm^3/g) [3]. This alloy becomes soft after the usual heat treatment, which is hardening from a temperature of 1150–1250 °C and rapid cooling. To achieve the desired hardness, the alloy after quenching is subjected to aging at temperatures of the order of 650 °C.

According to [4], during aging, the γ-solid solution decomposes with the precipitation of the Ni_3Al intermetallic compound and the α-Cr phase. Moreover, the volume content and distribution mainly along the boundaries or in the grain body of the α-Cr phase in the quenched state affects the processes of decomposition and the ratio of the volume fractions of the precipitated phases: the α-phase and the intermetallic phase. However, it is known (Fig. 1) that the Ni–Cr system contains an ordered $CrNi_2$ phase that exists at temperatures below ~ 590 °C (863 K). The composition of the 40HNU alloy is marked with a vertical dotted line.

It is generally accepted [6, 7] that the 40HNU alloy is nonmagnetic. However, we have previously discovered the appearance of magnetization in this alloy [8]. A connection was shown between the magnetic properties of this alloy, its structure and mechanical properties. It was shown in review [9] that the enhancement of ferromagnetic properties can be associated with the distortion of the crystal lattice, the presence of uncompensated magnetic moments of ions on the surface of magnetic particles, and defects. Studies of the 40HNU alloy presented in [10] show that quenching from 1050 °C (5 min) + rolling with $\varepsilon = 90\%$ with subsequent high-temperature stretching ensures the occurrence of superplasticity of the alloy in the range of strain rates 10^{-4}–10^{-2} s^{-1}, and in the temperature range 850–1050 °C. The main indicators of the superplasticity of the 40HNU alloy, namely, the parameter of flow stress sensitivity to the strain rate $m > 0.6$ and relative elongation after rupture $\delta > 1600\%$ reach maximum values at $T = 950 \div 1000$ °C and strain rate $\varepsilon \approx 9.3 \cdot 10^{-3}$ s^{-1}. It follows from the data obtained

✉ Fedor M. Noskov
fnoskov@sfu-kras.ru

[1] Siberian Federal University, Krasnoyarsk, Russia

[2] East Kazakhstan University named after S. Amanzholov, Ust-Kamenogorsk, Kazakhstan

[3] Kirensky Institute of Physics, Federal Research Center KSC SB RAS, Krasnoyarsk, Russia

Published online: 05 May 2023

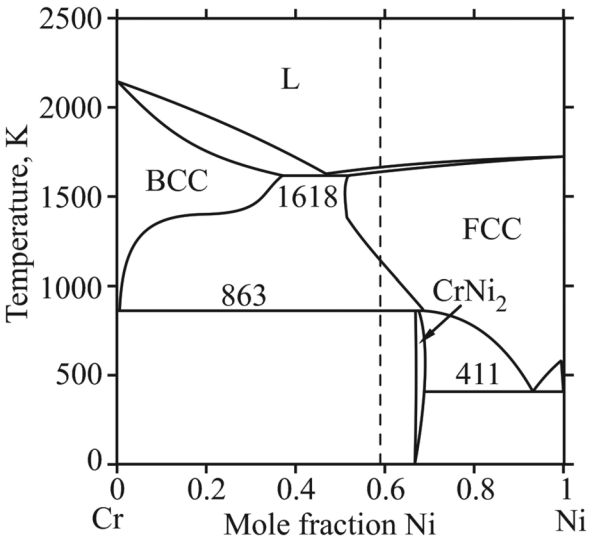

Fig. 1 State diagram of Ni–Cr [5]

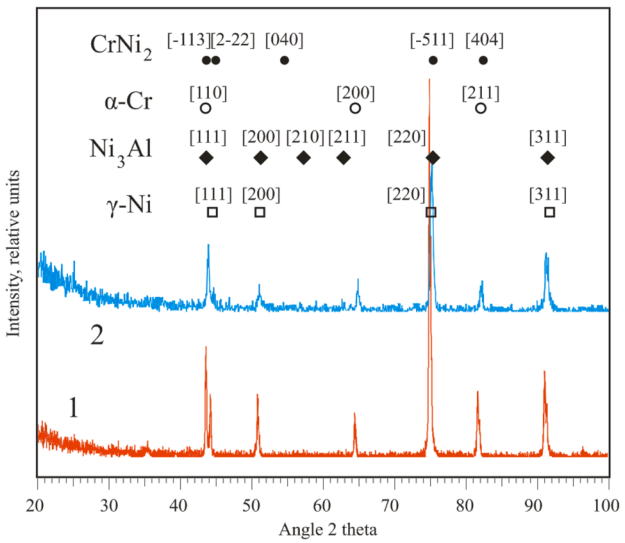

Fig. 2 Comparison of X-ray diffraction spectra of 40HNU alloys: 1—after quenching from 1250 °C and aging at 700 °C, without superplastic deformation; 2—with following superplastic deformation at 1000 °C

in [10, 11] that the 40HNU alloy reveals superplasticity at a relatively low flow stresses (5–40 MPa), which is general characteristic of superplastic flow.

Aim of the work: to investigate the phases, microstructure, magnetic properties, and mechanical properties in a Cr-Ni–Al alloy 40HNU after thermal treatment and severe (superplastic) deformation.

Tasks of the work: (1) X-ray diffraction method to investigate the phase composition and texture of samples before and after severely (superplastic) deformation. (2) To investigate the dependence of microhardness and coercive force in samples not subjected to a severely deformed sample on temperature and aging time. (3) To investigate the effect of a severe deformation on the structure and magnetic state of the alloy. (4) To reveal the nature of the appearance of magnetic properties in the alloy 40HNU.

2 Materials and Methods

Samples of the 40HNU alloy of vacuum induction melting were taken for the study. The content of the main elements in the alloy was (% by weight): Cr 39.5; Al 3.75; C 0.015, the rest Ni. After quenching from temperature of 1250 °C in water, the specimens were subjected to rolling with a reduction of 90%. As a result, a cold-rolled strip with a thickness of 0.1–0.3 mm was obtained. After quenching and deformation, the samples were subjected to aging with different durations in the range of 400–800 °C. Plates 0.3 mm thick obtained after treatment (quenching at 1250 °C, rolling at 90%, aging at 700 °C) were subjected to superplastic tension at a temperature of 1000 °C. The relative elongation δ after fracture was 400%.

Structural studies of the samples were carried out on a Hitachi TM4000 electron microscope with a microanalyzer. The phase composition of the alloy was determined by the X-ray diffraction method on a Bruker diffractometer using copper radiation. The microhardness was measured on a PMT-3 instrument at a load of 0.98 N. Magnetic characteristics, including coercive force, were measured on a torsional magnetometer in fields up to 1 T.

3 Results

The X-ray diffraction patterns of the samples after different treatments are shown in Fig. 2. The study confirms (spectrum 1) that the 40HNU alloy after heat treatment is characterized by the presence of a nickel-based FCC γ-solid solution with a lattice period $a = 0.355$ nm and chromium-based α-phase particles having a BCC lattice with $a = 0.287$ nm. Precipitates of the γ'-phase (Ni_3Al) are also present.

Since the sample was subjected to plastic deformation by rolling after quenching, before aging, it is quite natural that the texture [22] is observed in the X-ray diffraction pattern (Fig. 2, curve 1). After superplastic deformation, a texture associated with the appearance and growth of intermetallic phases appears in the sample in the same area of diffraction angles (Fig. 2, curve 2). Thus, it can be seen that during superplastic deformation, intermetallic phases grow in the form of thin secretions in the grain boundaries, which can lead to the appearance of unidirectional magnetic anisotropy.

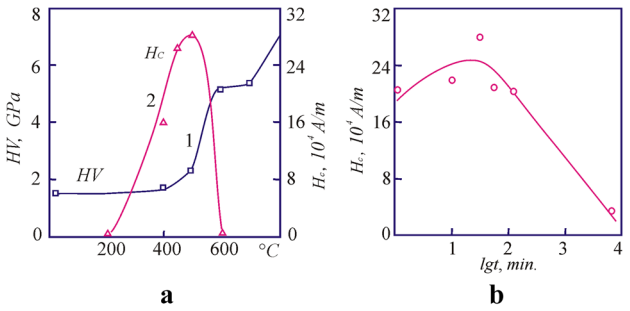

Fig. 3 Properties of the 40HNU alloy: **a** microhardness (1) and maximum coercive force (2) on the aging temperature. Aging time: 1—5 h; 2—variable, corresponding to the maximum value of H_c; **b** change in the coercive force of the alloy depending on the holding time at 500 °C

After aging of hardened specimens in the range of 350–400 °C for a long time, the structure of the alloy practically does not differ from the structure of hardened specimens. The first signs of decomposition are found after aging at 450 °C (Fig. 3a), and the decomposition of the γ-solid solution occurs according to the mechanism of discontinuous precipitation of the incoherent α-phase. The discontinuous decomposition reaches its highest intensity at 700 °C, while in the cells of discontinuous decomposition, simultaneously with the precipitation of the α-phase, the precipitation of the coherent γ'-phase (of the Ni_3Al type) also occurs.

When quenching from 1250 °C, the maximum microhardness is in the aging temperature range of 600–700 °C (Fig. 3a, curve 1). The coercive force (Fig. 3a, curve 2) has the highest value, corresponding to the maximum hardness for a hardening temperature of 1150 °C. The change in the coercive force is associated with a change in the size of the released single-domain ferromagnetic particles of intermetallic phases.

As the aging temperature increases, coercivity H_c increases, reaching a maximum at 500 °C (Fig. 3a, curve 2). According to the phase diagram (Fig. 1), at temperatures above 138 °C, the pure nickel phase is not formed; for these conditions, H_c should be equal to zero. However, a non-zero coercive force is observed in the samples. This may indicate precipitation during rolling and subsequent aging of ferromagnetic particles. X-ray diffraction analysis shows the presence of γ-Ni. It can be assumed that during plastic deformation and subsequent aging, the concentrations of chromium and alloying components in the solid solution were redistributed, and ferromagnetic particles enriched in nickel were formed. This phenomenon was directly observed in our work [8]. After aging at 500 °C and subsequent cooling to room temperature, the coercive force has the highest value (Fig. 3a). The following drop in H_c with increasing aging temperature is apparently associated with the enrichment of nickel particles with chromium.

Figure 4a shows an electron microscopic dark-field image taken using the nickel (111) reflection from a sample obtained by quenching from 1250 °C and aging at 450 °C. Dispersed nickel particles are visible. Note that in Fig. 4, large nickel precipitates are actually agglomerations of individual particles with a smaller size (which makes it difficult to analyze their sizes). Figure 4b shows a histogram of the distribution of nickel particles over the average diameter in the specified sample, made from a series of images. It can be seen from the figure that after annealing at 450 °C, about 85% of the nickel particles are smaller than 30 nm. Such a

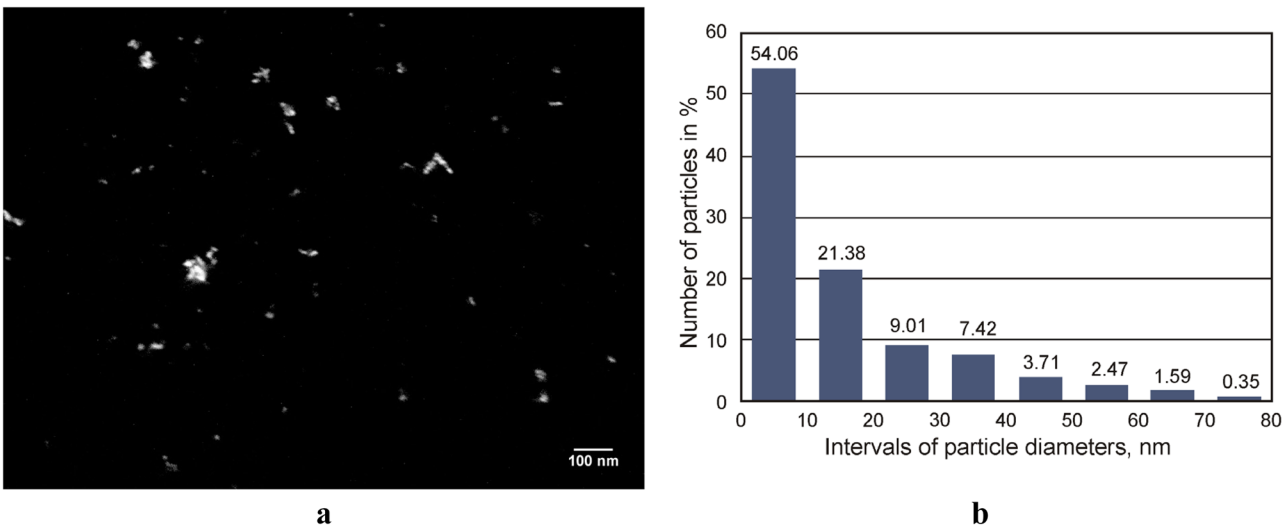

Fig. 4 Nickel particles in the 40HNU alloy after quenching and aging: **a** dark-field electron microscopic image obtained in the light of the (111) reflection of nickel after aging at 450 °C; **b** distribution histograms of average diameters of nickel particles after aging at 450 °C

Table 1 Composition of spectra from Fig. 5b

Spectrum number	Al, ат.%	Cr, ат.%	Fe, ат.%	Ni, ат.%	The phase to which the composition corresponds
1	7.33	32.28	0.37	60.02	$CrNi_2$
2	0.32	94.26	–	5.43	α-Cr
3	4.69	46.56	0.33	48.42	γ-Ni
4	1.39	83.64	0.18	14.78	α-Cr

size is close to the single domain size in nickel (~ 50 nm [15, 16]).

It makes observed maximal values of H_c in Fig. 3a clear. The following drop in H_c with increasing aging temperature up to 600 °C is apparently associated with the enrichment of nickel particles with chromium that makes it nonmagnetic.

Table 1 indicated spectrum 2 of the 40HNU alloy after heat treatment (quenching, rolling, and aging at 700 °C) and then subjected to superplastic tension at a temperature of 1000 °C is shown in Fig. 2 also. The alloy demonstrated the superplastic elongation δ about 400%. From a comparison of the two spectra in Fig. 2, it can be seen that as a result of superplastic deformation in the alloy, the quantitative ratio of α and γ phases has changed, and the $CrNi_2$ phase is also detected in a relatively small amount.

After superplastic deformation, the structure of the stretched zone in the region of sample rupture was studied using a scanning electron microscope using the option of element microanalysis. The results are shown in Fig. 5 and in Table 1. It can be seen that in the discontinuity zone, the matrix phase is a $CrNi_2$ intermetallic compound. It contains α-Cr particles, which have high hardness and were crushed during superplastic deformation (Fig. 5). It is interesting that in the zone of superplastic deformation, there are regions whose composition and structure correspond to the high-temperature eutectic (the transformation temperature is 1345 °C (1618 K), see Fig. 1). This may indicate the liquid-like behavior of the alloy during superplastic flow.

The magnetic properties in the sample after severe (superplastic) deformation were investigated using a torsional magnetometer. A sample in the form of a plate weighing 0.7903 g was measured. The field orientation ($H = 1$ T) was counted from the perpendicular to the plate (see the sketch in Fig. 6).

The magnetic energy of the sample $E(\theta, \varphi)$ in an external field H, taking into account two main possible contributions to the energy of magnetic anisotropy—uniaxial and unidirectional—is as follows:

$$E(\theta,\phi) = -M_s H\cos(\theta-\phi) - K_1\cos(\phi-\phi_1)^2 - K_0\cos(\phi-\phi_0) \quad (1)$$

where M_s is the saturation magnetization; K_1 and K_0 are the constants of uniaxial and unidirectional anisotropy, respectively; φ_1 and φ_0 are the angles corresponding to the direction of the anisotropy axes.

In equilibrium,

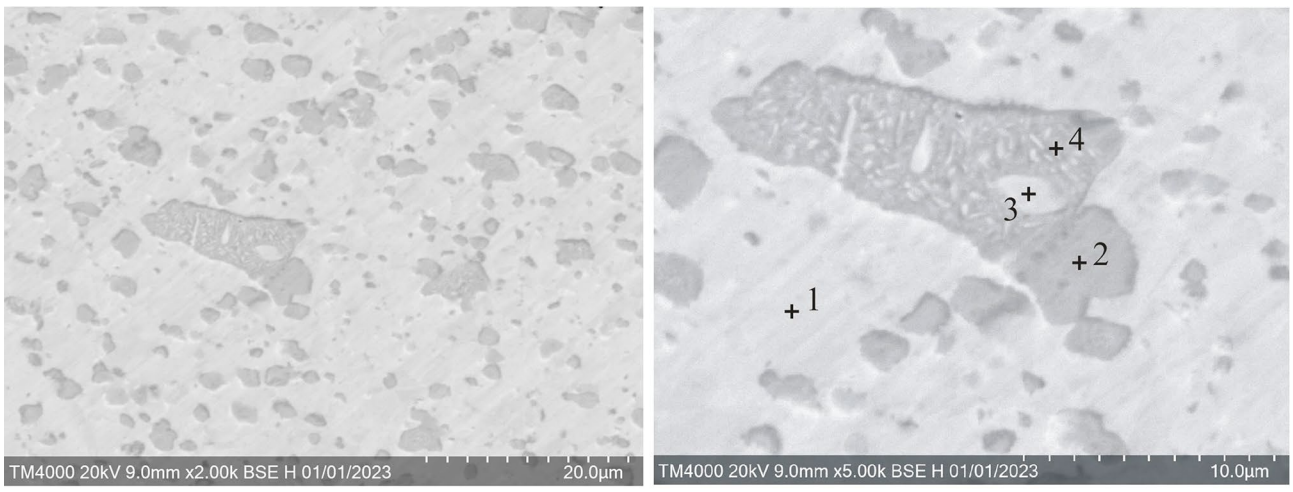

Fig. 5 Electron microscopic image of the 40HNU alloy section near the rupture after superplastic deformation at 1000 °C: **a** the general pattern of the microstructure; **b** the shooting locations of the diffraction spectra presented in

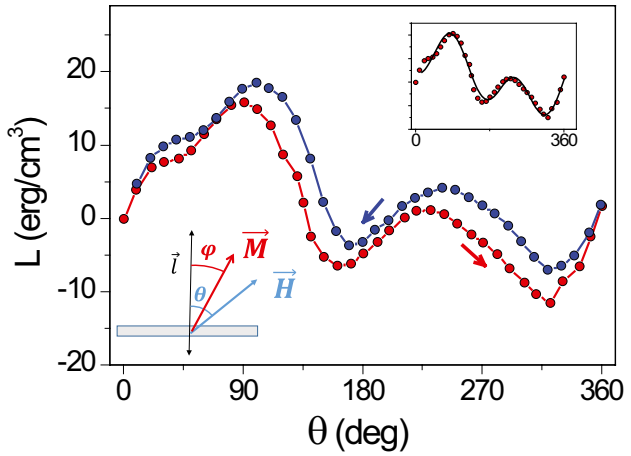

Fig. 6 Torque at different field directions. The inset shows the fitting of the experimental data by Eq. (3)

$$\frac{\partial E}{\partial \phi} = -M_s H \sin(\theta - \phi) - 2K_1 \sin(2\phi - 2\phi_1) - K_0 \sin(\phi - \phi_0) = 0 \tag{2}$$

Considering that torque $L = M_s H \sin(\theta - \varphi)$, and also the fact that in high fields (the field used in the measurement was 1 T) $\theta \approx \varphi$, we obtain

$$L(\theta) \approx -K_1 \sin(2(\theta - \theta_1)) - K_0 \sin(\theta - \theta_0) \tag{3}$$

The quality of fitting the angular dependence of the torque using Eq. (3) (see the inset in Fig. 6) shows that taking into account two contributions to the anisotropy is sufficient. The values of the parameters corresponding to the best fit were $K_1 = -12.9 \pm 0.8$ erg/cm^3, $K_0 = 7.9 \pm 0.4$ erg/cm^3, $\theta_1 = 11 \pm 4$ deg, $\theta_0 = -66 \pm 14$ deg.

4 Discussion

X-ray diffraction analysis and electron microscopic observations of the 40HNU alloy after quenching and aging made it possible to establish that, starting from 400 °C, inside the primary particles of the γ-phase (a solid solution of chromium in nickel), the supersaturated solid solution decomposes. The particles of the new phase released during the decomposition (Fig. 2) are the coherent γ'-phase (of the Ni_3Al type), as well as the almost pure nickel. According to the phase diagram of the Ni–Cr system, nickel particles precipitate in the α-phase (Fig. 1), but this is possible under equilibrium conditions in an alloy with a nickel content that exceeds its amount in the alloy under study. However, the processing conditions (quenching, rolling, aging, and especially the severe deformation) were far from equilibrium, and a small amount of pure nickel could precipitate in localized areas as a result. This can be associated with a lower barrier for the nucleation of nickel particles than particles of the $CrNi_2$ phase and is due to a smaller mismatch between the lattice parameters of the γ phase and nickel in comparison with the mismatch between the parameters of the γ phase and $CrNi_2$.

To eliminate the undesirable magnetic properties of the 40HNU alloy, it can be recommended to increase the upper quenching temperature to 1250 °C, which shifts the maximum strength properties to aging temperatures of 600–700 °C, at which the alloy is nonmagnetic.

The presence of Ni_3Al in the 40HNU alloy is shown in [4]. Available data on the magnetic state of the Ni_3Al phase are contradictory. It is shown in [12] that, in atomically ordered Ni_3Al, the magnetization is low and weakly depends on the degree of atomic order. In [13], it was demonstrated that high-temperature deformation of high-temperature nickel alloys increases the values of magnetic susceptibility due to atomically ordered Ni_3Al clusters. The authors of [14] report the instability of these clusters, which recrystallize during thermal and deformation treatment, and the magnetic order is destroyed. Thus, the contribution of the Ni_3Al phase to the magnetization of the 40HNU alloy cannot be significant.

It is known that the coercive force H_c depends on the structural and phase state of the alloy; therefore, it was interesting to understand whether it is possible that small amount of nickel inclusions would be responsible for the formation of the ferromagnetic properties in the heat-treated 40HNU alloy.

The observed coercive force (over 8×10^4 A/m) is high even in comparison with the nickel magnetocrystalline anisotropy field (2×10^4 A/m) [15]. This can be related to the fact that nickel precipitates in the γ-phase not only have a size of the order of several tens of nanometers, close to the nickel single-domain size, but are also in a stressed state. If the nickel particle size becomes smaller than the critical one, then these particles become superparamagnetic and the coercive force decreases [16].

The authors of [17] believe that the presence of the $CrNi_2$ ferromagnetic phase may imply a higher magnetization of the alloy containing this phase. However, in the same work, it is shown that $CrNi_2$ can form an antiferromagnetic structure, which is destroyed at temperatures above 550 K with minimal effect on the chemical bond. The paper discusses the relationship between the magnetic phase transition and the transition to the chemically ordered structure of $CrNi_2$. An extremely low temperature for chemical rearrangement was found at an experimental heating rate of 100 K/h. It is known that unidirectional magnetic anisotropy arises in materials having a defect antiferromagnetic structure [9]. Such an effect can reveal itself as a result of the appearance of a fine texture of the deformed material. This makes it possible to relate the nature of the magnetic rotational hysteresis shown in Fig. 6 with the results of electron microscopic

studies (Fig. 5), which showed that in the zone of superplastic deformation, the matrix phase corresponds to the composition $CrNi_2$ (Table 1), which is apparently atomically disordered.

The magnitude of the angles and the signs of the anisotropy constants, taking into account the presence of hysteresis in Fig. 6, fitting errors and angle control errors, allows us to say that both anisotropy axes are orthogonal to the plane of the measured plate. The negative sign of K_1 means that the uniaxial anisotropy is an anisotropy of the easy plane type, which can naturally be attributed to the magnetic anisotropy of the plate shape. If the sample structure is represented as a composite (nickel inclusions in a Cr-Ni matrix), the K_1 value can be used to estimate the volume fraction of Ni inclusions using the equation $K_1 = 2\pi\nu {M_s}^2$. Assuming $M_s = 500$ G (nickel), we have the estimate $\nu = \frac{K_1}{2\pi M_s^2} = 8 \cdot 10^{-6}$. Based on the fact that a small fraction of pure nickel inclusions can form in the composition of 40HNU, we can quantify their fraction using the leverage rule, and by this calculation, we can (potentially) estimate the amplitude of composition fluctuations. Such work is expected in the near future.

The unidirectional anisotropy constant is also very small; however, such anisotropy itself can be associated both with the flexomagnetic effect induced by plastic deformation and, for example, with the bonding of nickel inclusions with the antiferromagnetic or weakly ferromagnetic $CrNi_2$ matrix. An additional argument in favor of the existence of an exchange coupling between $CrNi_2$ and nickel inclusions can be a noticeable torque hysteresis. The point is that the field of 1 T used in measuring the curve given in Fig. 6 is too large compared to the nickel magnetocrystalline anisotropy field. The exchange coupling between a ferromagnetic grain and an antiferromagnetic matrix (see, for example, [18, 19]) can lead to magnetic hysteresis in very high fields.

Figure 5 showed that centers with eutectic structure are observed in the superplastic deformation zone (Table 1 is compared with the diagram in Fig. 1). This can explain the superplastic behavior of the alloy, which experiences a transition to a liquid-like state in localized zones during severe deformation. After the finish of the deformation process, these regions form "crystallized" eutectic regions. The model of super-Arrhenius relaxation makes it possible to explain the liquid-like behavior during superplastic deformation as the movement of shear transformation zones in different parts of the loaded sample (Fig. 5). In localized regions of alloys with energy density gradients, the driving force of dynamic processes is the temperature and concentration gradient [20]. According to the model of excited atoms and a shear transformation zone, the driving force of the process can be the pressure arising from internal stress fluctuations even under a small temperature effect [21, 22].

5 Conclusions

1. The ferromagnetic properties of the 40HNU alloy are associated with the precipitation of nickel in the primary particles of the γ-phase. The drop in the coercive force down to zero during isothermal annealing is explained by the enrichment of nickel particles with chromium.
2. It is shown that the $CrNi_2$ phase can be formed in the zone of superplastic deformation as a matrix phase, while the regions with eutectic structure are observed in the localized zones.
3. The appearance of unidirectional magnetic anisotropy in 40HNU alloy samples after superplastic deformation can be attributed to the antiferromagnetic structure of $CrNi_2$.
4. An increase in the quenching temperature before aging leads to the elimination of undesirable magnetic phenomena in the alloy while maintaining a high level of strength properties.

Acknowledgements The authors express their gratitude to Nurgamit Kantay (East-Kazakhstan University named after S. Amanzholov) for his help in conducting the experiment.

Author Contribution Conceptualization: L.I.K., F.M.N., and S.V.K.; methodology: L.I.K., M.N.V., and S.V.K.; software: S.V.K. and M.N.V.; validation: L.I.K. and D.E.Y.; formal analysis: L.I.K., F.M.N., and S.V.K.; investigation: L.I.K. and M.N.V.; resources: D.E.Y.; data curation: F.M.N. and S.V.K.; writing—original draft preparation: L.I.K. and F.M.N.; writing—review and editing: S.V.K. and L.I.K.; visualization: F.M.N. and S.V.K.; supervision: L.I.K.; project administration: F.M.N.; funding acquisition: F.M.N. and L.I.K. All authors have read and agreed to the published version of the manuscript.

Data Availability The data that support the findings of this study are available from the corresponding author upon reasonable request.

Declarations

Consent to Participate Not applicable.

Conflict of Interest The authors declare no competing interests.

References

1. Uwatoko, Y., Todo, S., Ueda, K., Uchida, A., Kosaka, M., Mori, N., Matsumoto, T.: Material properties of Ni–Cr–Al alloy and design of a 4 GPa class non-magnetic high-pressure cell. J. Phys. Cond. Matter **14**, 11291 (2002)
2. Sadykov, R.A., Bezaeva, N.S., Kharkovskiy, A.I., Rochette, P., Gattacceca, J., Trukhin, V.I.: Nonmagnetic high pressure cell for magnetic remanence measurements up to 1.5 GPa in a superconducting quantum interference device magnetometer. Rev. Sci. Instrum. **79**(11), 115102 (2008). https://doi.org/10.1063/1.2999578. PMID: 19045908
3. Sadykov, R.A., Litvin, V.S., Kharkovsky, A.I., Appavou, M.S., Ioffe, A.: Research of 40HNU alloy annealing kinetics by small

angle neutron scattering The Fourth International Conference «Deformation & Fracture of Materials and Nanomaterials» (DFMN -2011) 25–28 Oct., Moskow, Russia, p. 850–852. (2011)
4. Yakovleva, S.A., Shcherbak, A.G.: Investigation of the influence of heat treatment modes on the structural-phase state of the alloy 40HNU-vi // Scientific and Technical Bulletin of the St. Petersburg State University of Information Technologies, Mechanics and Optics, № 5(75), p. 96–100. (2011)
5. Hao, L., Ruban, A., Xiong, W.: CALPHAD modeling based on Gibbs energy functions from zero kevin and improved magnetic model: a case study on the Cr–Ni system. Calphad **73**, 102268 (2021)
6. Knyazeva, G.G., Krasnopevtseva, T.V., Paretskaya, R.M.: A new non-magnetic stainless alloy with high hardness and wear resistance. In the book: Precision alloys Metallurgy: Moskow, Russia, issue 78, pp. 134-140. (1971)
7. Molotilov, B. M.: Precision alloys. 448 p. Moscow: Metallurgy (1974)
8. Petrov, V.A., Sukhovarov, V.F., Kveglis-Vershinina, L.I.: Magnetic properties of alloy 40 HNU-VI. Phys. Met. Metall. **56**(1), 47–52 (1983)
9. Pyatakov, A.P., Zvezdin, A.K.: Magnetoelectric and multiferroic media. Phys. Usp. **55**, 557–581 (2012). https://doi.org/10.3367/UFNe.0182.201206b.0593
10. Radashin, M.V., Radchenko, O.A., Sukhovarov, V.F., Petrov, V.A.: Superplasticity of alloy 40HNU and its use in the production technology of elastic elements of devices 1st Rep. conf. "Solid state physics and new areas of its application" Karaganda, Kazakhstan, p.35. (1986)
11. Grebneva, B.C., AlontsevaIO D.L., Ivanov, A.A.: Optimal temperature-speed regime of superplasticity of alloy 40HNU Materials of the II Republican Scientific and Technical Conference "Scientific and technical progress: quality management, energy and resource conservation on the threshold of the XXI century", Part I. Ust-Kamenogorsk, Kazakhstan; p. 52–54. (2001)
12. Sob, M., Leguta, D., Friák, M., Fiala, J.: Magnetism of Ni_3Al and Fe_3Al under extreme pressure and shape deformation: an ab initio study. J. Magn. Magnet. Mater. **272–276**, E205–E206 (2004)
13. Felcher, G.P.: Magnetic moment distribution in Ni_3Al. AIP Conf Proc **29**, 285 (1976). https://doi.org/10.1063/1.30632
14. Chen, Y., Prasath babu, R., Slater, T.J.A.: An investigation of diffusion-mediated cyclic coarsening and reversal coarsening in an advanced Ni-based superalloy. Acta Mater. **110**, 142 (2016)
15. Chikazumi, S.: Physics of ferromagnetism. 668 p. Oxford University Press (2009)
16. Kondorsky, E.I.: Micromagnetism and remagnetization of quasi-one-domain particles. Izv of the USSR Academy of Sciences, Ser. Phys. **42**(8), 1638–1648 (1978)
17. Walsh, F., Ritchie, R.O., Asta, M.: Theoretical antiferromagnetism of ordered face-centered cubic Cr-Ni alloys. Phys. Rev. Mater. **6**(11), 113602 (2022)
18. Kodama, R.H., Berkowitz, A.E., McNiff, E.J., Foner, S.: Surface spin disorder in $NiFe_2O_4$ nanoparticles. Phys. Rev. Lett. **77**, 394–397 (1996). https://doi.org/10.1103/PhysRevLett.77.394
19. Kodama, R.H.: Magnetic nanoparticles. J. Magn. Magn. Mater. **200**, 359–372 (1999). https://doi.org/10.1016/S0304-8853(99)00347-9
20. Langer, L.S.: Dynamics of shear-transformation zones in amorphous plasticity: formulation in terms of an effective disorder temperature. Phys. Rev. E **70**, 041502 (2004)
21. Falk, M.L., Langer, J.S.: Shear transformation zone theory elasto-plastic transition in amorphous solids. Phys. Rev. **E57**, 7192–7204 (1998)
22 Lemaitre, A., Carlson, J.: Boundary lubrication with a glassy interface. Phys Rev. E **69**, 061611(1–8) (2004)